



Original Article

Multidetector Computed Tomography Findings of Auto-Evacuated Secondary Acquired Cholesteatoma: A Morphologic and Quantitative Analysis

İrfan Çelebi , Gülpenbe Bozkurt , Abdullah Soydan Mahmutoğlu , Umman Guliyev 

Department of Radiology, Şişli Hamidiye Etfal Training and Research Hospital, İstanbul, Turkey (İÇ, UG)

Department of Otorhinolaryngology, Acıbadem University Hospital, İstanbul, Turkey (GB)

Department of Radiology, İstanbul Training and Research Hospital, İstanbul, Turkey (ASM)

ORCID IDs of the authors: İ.Ç. 0000-0003-2562-2482; G.B. 0000-0003-2100-023X; A.S.M. 0000-0001-7987-0006; U.G. 0000-0002-3237-8687.

Cite this article as: Çelebi İ, Bozkurt G, Mahmutoğlu AS, Guliyev U. Multidetector Computed Tomography Findings of Auto-Evacuated Secondary Acquired Cholesteatoma: A Morphologic and Quantitative Analysis. J Int Adv Otol 2018; 14(3): 464-71.

OBJECTIVES: To describe and quantify computed tomography (CT) findings of auto-evacuated (spontaneously drained) secondary acquired cholesteatoma (SAC).

MATERIALS and METHODS: This multicenter retrospective study included 69 patients with intermittent ear discharge diagnosed with SAC by otoscopy or otomicroscopy who were surgically treated. Three independent radiologists measured the medial and lateral attic distance on coronal and axial planes using multidetector computed tomography (MDCT) in 75 ear CTs from 69 patients with intraoperatively verified diagnoses of pars flaccida cholesteatoma (n=36), pars tensa cholesteatoma (n=24), and auto-atticotomy or automastoidectomy (n=15) and compared them with contralateral healthy ears.

RESULTS: A circular or elliptical air-filled cavity surrounded by granulation tissue was morphologically detected on MDCT in these patients. The lateral attic distance was significantly higher in pars flaccida cholesteatoma cases than in contralateral healthy ears on both coronal and axial planes ($p<0.05$). The medial attic distance was significantly higher in pars tensa cholesteatoma cases than in contralateral healthy ears in the axial plane, but with no difference in the coronal plane.

CONCLUSION: In patients with chronic intermittent aural discharge, nonopacified areas surrounded by granulation tissue, which expands the medial or lateral attic in a CT scan, suggest an auto-evacuated cholesteatoma.

KEYWORDS: Cholesteatoma, computed tomography, aural discharge, diagnosis, attic distance

INTRODUCTION

A cholesteatoma is a benign but clinically destructive lesion histologically described as a well-demarcated cystic mass formed from the keratinizing stratified squamous epithelium^[1-3]. Surgical resection is the only treatment option for removing cholesteatomas from the middle ear^[3-8].

The diagnosis of cholesteatoma is based on the clinical signs and symptoms, primarily discharge and conductive hearing loss due to the mechanical compression and/or erosion of adjacent structures by the lesion and hyperproliferative cells^[9, 10]. The clinical diagnosis of cholesteatomas is supported by computed tomography (CT) scans showing bone erosion or destruction, which differentiates cholesteatoma from granulation tissue or fluid retention due to chronic otitis media. The typical CT findings of cholesteatomas are a soft-tissue mass in the middle ear cavity with varying levels of destruction^[2, 3, 7, 11]. However, in clinical practice, CT may sometimes show a spontaneously evacuated, nonopacified spontaneously drained auto-evacuated secondary acquired cholesteatoma (SAC) associated with an extensive osseous wall destruction of the middle ear, which has been discussed in literature^[12-16]. A drained, nonopacified SAC that is associated with marked destruction of the ossicles or bony structures, indicates a mural cholesteatoma, also known as automastoidectomy or nature's mastoidectomy. In contrast, the term auto-atticotomy or nature's atticotomy, which is less extensive and destructive than automastoidectomy, is used to describe a smaller defect where only the scutum and lower lateral attic wall are affected^[1, 16].

Corresponding Address: İrfan Çelebi E-mail: irfancelebidr@hotmail.com

Submitted: 21.11.2017 • Revision Received: 05.02.2018 • Accepted: 05.03.2018 • Available Online Date: 15.10.2018

©Copyright 2018 by The European Academy of Otolology and Neurotology and The Politzer Society - Available online at www.advancedotology.org

In this study, we aimed to describe and quantify the CT findings of auto-evacuated cholesteatoma, including nondestructive and non-opacified types verified by surgery.

MATERIALS and METHODS

Study Design and Population

We retrospectively reviewed the hospital discharge records of 191 patients who were operated for cholesteatoma between May 2014 and November 2017. In all the patients, the diagnostic criteria for SAC were chronic intermittent aural discharge associated with tympanic membrane perforation or a deep attic retraction pocket. Out of the 191 patients, 98 with typical CT signs of cholesteatoma (a destructive opacified mass in the middle ear); 15 with a history of ear surgery, including ventilation tube insertion and type 1 tympanoplasty; and nine with no evidence of cholesteatoma at surgery were excluded. Finally, we included 69 patients [21 females, 48 males; mean age, 45 (range: 17–74) years] with 75 ears with auto-evacuated SAC (six patients had bilateral SAC).

The study was approved by the Institutional Ethics Committee (No. 684; date, 06/21/2016), and the requirement for informed consent was waived due to the retrospective study design.

Classification of SAC

We classified auto-evacuated SAC into pars flaccida (attic or Prussak’s space cholesteatoma), pars tensa (cholesteatoma with pars tensa perforation), consistent with the Barath classification [13], and a third ad hoc (undetectable) group comprising patients with auto-atticotomy or mural cholesteatoma, which is also known as automastoidec-tomy (Table 1).

Radiological Assessment

Preoperatively, all patients underwent temporal bone CT on a 128-section multidetector CT (MDCT) scanner (Somatom Definition AS Plus 128; Siemens, Forchheim, Germany). The parameters were 320 mA tube current, 120 kV; 128-0.625 detector collimation; 0.5 s rotation time; 1 mm/rotation (pitch 0.391) table speed; 0.67 mm slice thickness; 4.9 s scan time; 96 mm field of view; and 512×512 matrix. No medication was administered in the ear for 24 h before the examinations. The preoperative images were recorded on compact discs, which were then loaded as raw data into a Philips Brilliance ICT 256 (Philips Medical Systems, Best, The Netherlands) and evaluated on an Extended Brilliance Workspace (Philips Medical Systems, Best, The Netherlands) to reconstruct them in every plane and to simultaneously access them in three orthogonal planes (axial, sagittal, and coronal), while maintaining their original resolution. In this way, the optimal anatomical detail was obtained. The anatomical reference

points of both inner ears (lateral semicircular canals) could be lined symmetrically in the same plane for optimal quantitative measurements and an accurate comparison of both sides. The lateral semicircular canals were aligned to obtain complete circular images in the axial plane (Figure 1a), and assessments were made perpendicular to this alignment in the coronal plane (Figure 1b).

Postoperatively, three expert head and neck radiologists who were blinded to patients’ clinical and surgical data re-evaluated these temporal MDCT images with respect to ossicular and scutum erosion, tegmen tympani defect, labyrinthine fistula, posterior wall remodeling or erosion, opening of the eustachian tube, and sinus tympani.

The MDCT images were also quantitatively analyzed by measuring the lower lateral attic recess (i.e., the distance between the long process of the incus and the lateral attic wall) and upper medial attic recess (i.e., distance between the head of malleus and the medial attic wall) in two planes. To ensure this, the incudomalleolar joint was initially found in the axial plane; then, by moving caudally, the distance between the long process of the incus and the lateral attic wall was measured perpendicular to the attic wall at the exact level of the superior margin of the external ear canal (Figure 1c). Next, by moving cranially, the distance between the head of the malleus and the medial attic wall was measured perpendicular to the attic wall just above the facial canal tympanic segment (Figure 1d). The distances between the scutum and the long process of the incus and between the head of malleus and the medial attic wall (Figure 1e and 1f, respectively) were also measured in the coronal plane. The radiologists made quantitative measurements for either the diseased or healthy ears and did not communicate while taking the measurements.

Quantitative measurements could be made for 64 of the 75 ears with auto-evacuated SAC because there was no reference bone wall in 11 patients due to scutum or incudostapedial destruction. These measurements were compared with data from the contralateral healthy ears (63 ears) of 63 patients with unilateral disease.

Statistical Analysis

The Kolmogorov–Smirnov test was used to evaluate the distribution of continuous variables. The Wilcoxon signed-rank test was used for the analysis of paired data (repeated measurements). Statistical analysis was performed using the Statistical Package for Social Sciences for Windows software version 22.0 (IBM Corp.; Armonk, NY, USA). The level of statistical significance was set at $p < 0.05$.

RESULTS

The intraoperatively verified diagnoses of 69 patients (75 ears) were pars flaccida cholesteatoma for 36 ears, pars tensa cholesteatoma

Table 1. Intraoperatively confirmed diagnosis of 75 ears with auto-evacuated SAC (n=69 patients) according to the modified classification system of Barath et al. (2011)

SAC classification	Initial location of cholesteatoma	Number of ears (%)
Pars flaccida cholesteatoma (attic or Prussak’s space)	Epytympanum (lateral to ossicle)	36 (48.0%)
Cholesteatoma with pars tensa type perforation (sinus)	Mesotympanum (medial to ossicle)	24 (32.0%)
Ad hoc group (mural cholesteatoma/auto-atticotomy)	Undefined	15 (20.0%)
Total		75

SAC, secondary acquired cholesteatoma

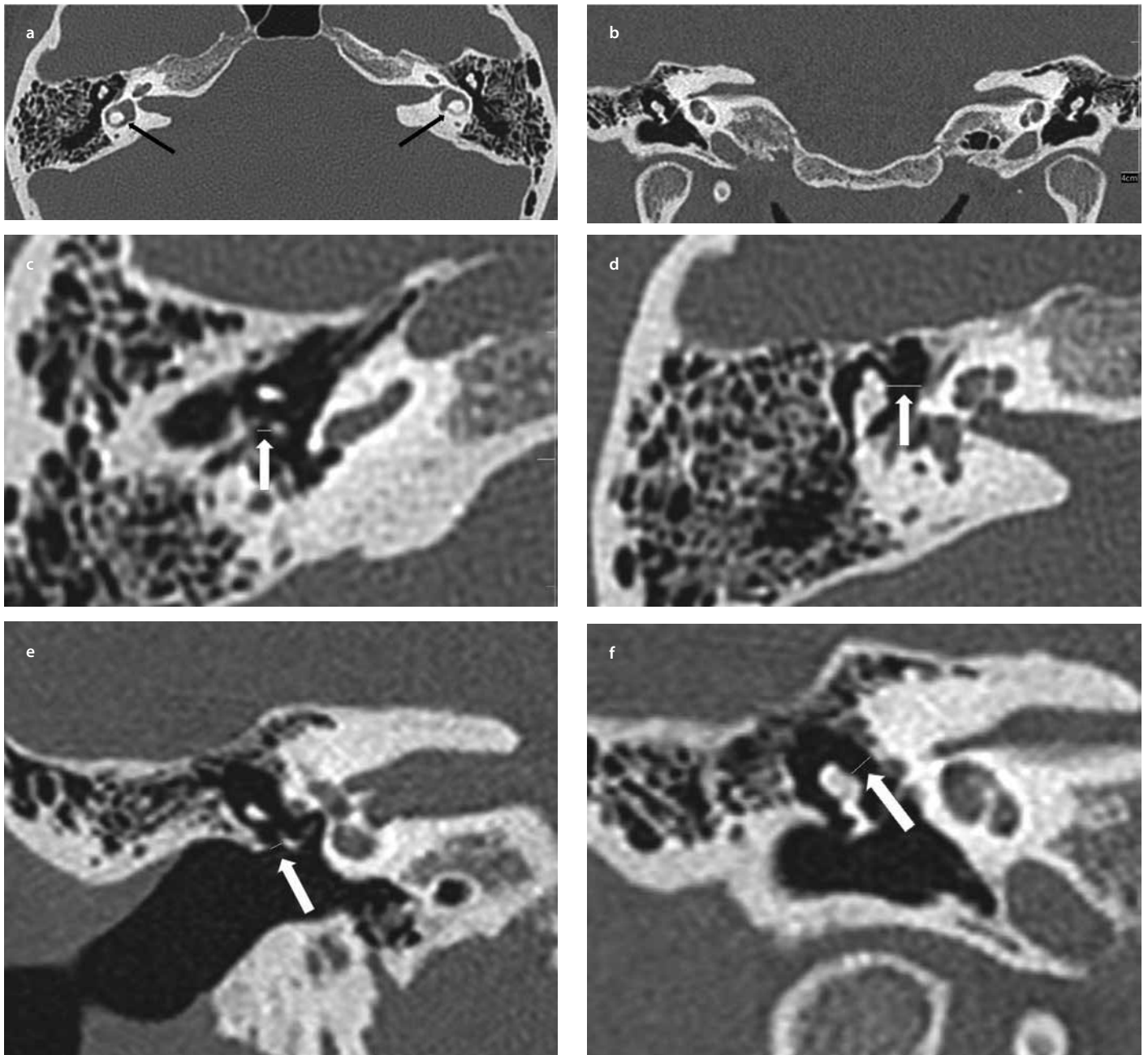


Figure 1. a-f. Axial (a) and coronal (b) MDCT images showing bilateral temporal bones symmetrically. In the axial image (c), the white thin line indicates the distance between the long process of incus and lateral attic wall. The axial image (d) shows the medial attic recess; the white thin line indicates the distance between the head of malleous and the medial attic wall. In the coronal image (e), the white thin line indicates the lateral attic distance between the scutum and the long process of incus. On the coronal image (f), the white thin line indicates the medial attic distance between the head of malleous and the medial attic wall.

for 24 ears, and auto-atticotomy or automastoidectomy for 15 ears (Table 1).

Morphological Evaluation on CT

Table 2 and Figure 2 summarize the morphological evaluations made on MDCT. Scutum blunting and total ossicular destruction were detected in six ears, wherein the middle ear was completely pneumatized. Minor ossicular erosion was detected in six ears with pars flaccida type cholesteatomas and three ears with the pars tensa type (12%) and was clearly observed because of the smooth bony remodeling on the posterior tympanic wall in all of these ears. In two ears with pars flaccida cholesteatoma (3%), there was no scutum or ossic-

ular destruction. Three patients had mastoid air cell aeration ipsilateral side. No or underpneumatization or opacification was detected in 72 (96%) of the 75 ears with cholesteatoma.

The most frequent CT finding in the partially or completely auto-evacuated SAC cases was a partially or completely empty circular or elliptical aerated cavity surrounded by granulation tissue (Figures 3 and 4). The wall structure of this circular or elliptical aerated cavity (matrix and perimatrix) of the cholesteatoma was almost never visualized because the thickness of the squamous epithelium was below the resolution limits of the device or it was obscured by the surrounding granulation tissue.

Table 2. Morphological findings on radiological evaluation with respect to cholesteatoma types

	Pars flaccida (n=36)	Pars tensa (n=24)	Auto-atticotomy mural cholesteatoma (n=15)	Total (n=75)
Posterior wall remodeling	22 (61 %)	20 (83 %)	12 (80 %)	54 (72 %)
Opening of eustachian tube	30 (83 %)	23 (95 %)	13 (86 %)	66 (88 %)
Ossicular erosion	28 (77 %)	20 (83 %)	15 (100 %)	63 (84 %)
Scutum erosion	22 (61 %)	14 (58 %)	15 (100 %)	51 (68 %)
Tegmen tympani defect	1 (2 %)	0 (0 %)	3 (20 %)	4 (5 %)
Opening of sinus tympani	22 (61 %)	11 (45 %)	5 (33 %)	38 (51 %)
Labyrinthine fistula	0 (0 %)	0 (0 %)	2 (13 %)	2 (3 %)

Table 3. Quantitative measurements on coronal and axial CT images of ears with auto-evacuated SAC and contralateral healthy ears

	CT plane	Ears with SAC			p*		
		Pars flaccida (n=32)	Pars tensa (n=24)	Auto-atticotomy mural cholesteatoma (n=8)	Healthy ears (n=63)	Pars flaccida vs. healthy ears	Pars tensa vs. healthy ears
Lateral attic (mm)	Coronal	2.56±0.76	1.40±0.86	4.3±1.2	1.20±0.22	<0.012	
	Axial	3.83±1.52	1.67±0.94	5.1±0.7	2.50±0.51	<0.012	
Medial attic (mm)	Coronal	2.36±0.44	2.92±0.91	1.7±1.1	2.52±0.77		>0.379
	Axial	2.02±0.68	3.42±1.00	1.0±0.8	2.41±0.74		<0.001

SAC: secondary acquired cholesteatoma; CT: computed tomography
 Data are given as mean±standard deviation
 *Wilcoxon signed-rank test

In pars flaccida cholesteatoma cases, lateral attic expansion and scutum erosion were determined in the coronal plane, whereas in pars tensa perforation cases (pars tensa cholesteatomas), medial attic expansion and posterior wall flattening (smooth remodeling) were best visualized in the axial plane. The recess expansions were confirmed by quantitative measurements.

Quantitative CT Measurements

Table 3 presents the quantitative measurements in the coronal and axial CT images of ears with auto-evacuated SAC and contralateral healthy ears. The distance of the lateral attic in ears with pars flaccida cholesteatoma in both coronal and axial planes was significantly higher than that in contralateral healthy ears (2.56±0.76 vs. 1.20±0.22 mm in the coronal plane, p=0.012; 3.83±1.52 vs. 2.50±0.51 mm in the axial plane, p=0.012). The distance of the medial attic was significantly higher in pars tensa cholesteatoma cases than in contralateral healthy ears in the axial plane (3.42±0.91 mm vs. 2.41±0.74 mm, p=0.001), with no difference in the coronal plane.

DISCUSSION

A cholesteatoma has three components: cystic contents comprising desquamated keratin, matrix, and perimatrix (with the last two also being known as the “shell”) [2, 17, 18]. Sometimes, an acquired cholesteatoma spontaneously evacuates into the external auditory canal, leaving a cavity (shell) within the granulation tissue in the shape of the original cholesteatoma, but now filled partially or totally with air, instead of exfoliated keratin, which appears opacified. This is called an auto-evacuated (spontaneously drained) SAC. Since the healthy middle ear is already filled with air, a drained SAC is difficult to radiologically evaluate if there is no major ossicular or scutum destruction.

In this study, we presented the CT findings of auto-evacuated cholesteatomas, which form a spherical or elliptical air cavity in which the peripheral wall of the cholesteatoma wall is surrounded by the granulation tissue, wherein some of them are nondestructive and unidentified so far.

The air-filled cavity of SAC consists of the peripheral cholesteatoma wall and is composed of keratinized squamous epithelium, which is the remnant of the cholesteatoma, i.e., the matrix and perimatrix or the so-called shell [12-16, 18]. This matrix wall continues its aggressive osteolytic activity and is seen on CT as a partially opacified or completely empty air-filled cavity, depending on how much of its contents have drained and the accumulation of keratin and epithelial debris [8, 19].

The enlargement of the lateral attic recess in pars flaccida and medial attic recess in pars tensa cholesteatomas causing ossicular and/or tympanic wall destruction is well known [1, 16, 20]. In some of our patients, we observed an increase in the lateral attic distance in auto-evacuated pars flaccida cholesteatomas without the presence of scutum or lateral attic wall erosion (Figure 3). We believe that an auto-evacuated cholesteatoma can be radiologically diagnosed within the granulation tissue before it forms a massive destructive cavity, such as automastoidectomy or auto-atticotomy. As such, a nondestructive spontaneously evacuated SAC can be an early sign of auto-atticotomy or automastoidectomy.

According to our experience in patients with pars tensa cholesteatoma, a slight medial attic expansion may be easily underestimated in the coronal plane. Therefore, we recommend that the axial plane

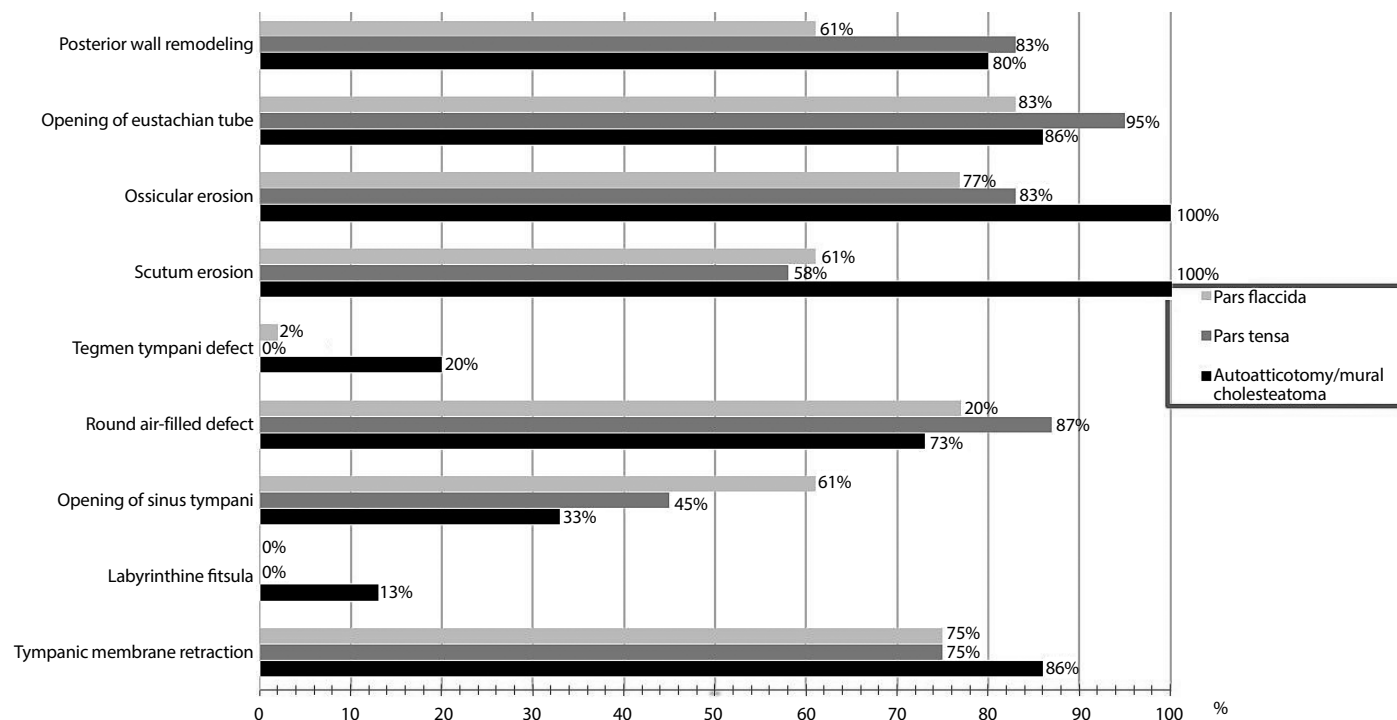


Figure 2. Percentage of morphological findings with respect to cholesteatoma types on radiological evaluation.

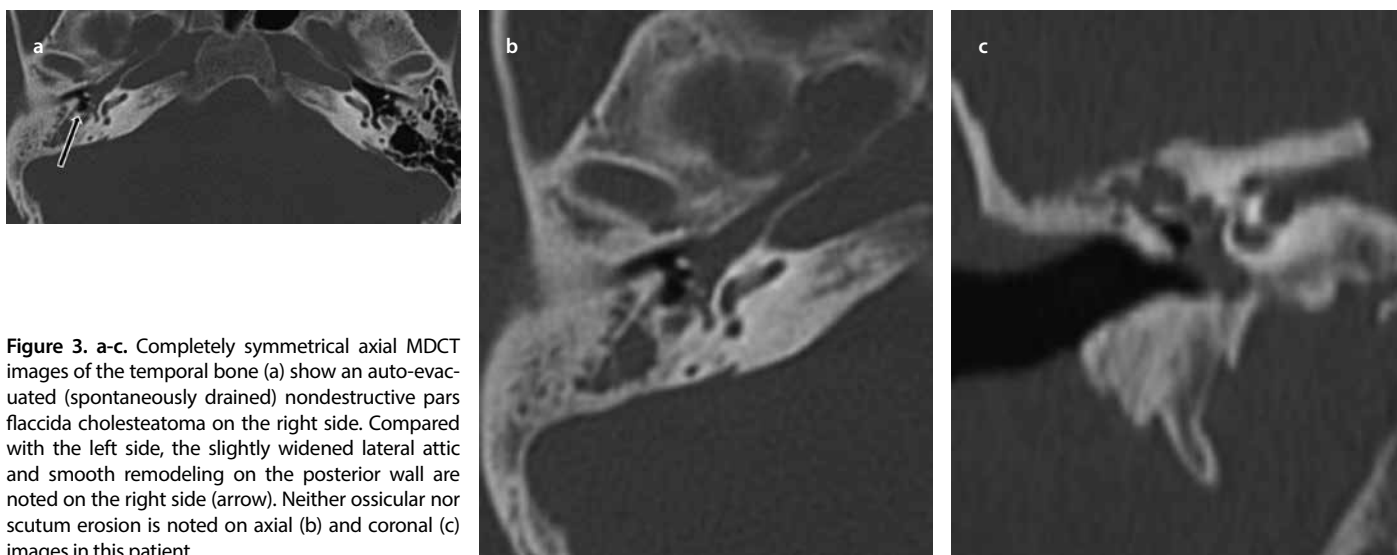


Figure 3. a-c. Completely symmetrical axial MDCT images of the temporal bone (a) show an auto-evacuated (spontaneously drained) nondestructive pars flaccida cholesteatoma on the right side. Compared with the left side, the slightly widened lateral attic and smooth remodeling on the posterior wall are noted on the right side (arrow). Neither ossicular nor scutum erosion is noted on axial (b) and coronal (c) images in this patient.

evaluation in these patients should be always made. We additionally observed smooth bony remodeling of the posterior tympanic wall in the axial plane in addition to lateral or medial attic enlargement (Figure 3-6). This finding can also support the diagnosis in more complex questionable cases.

The opacified appearance of a nondestructive cholesteatoma cannot be easily differentiated from the surrounding granulation tissue, fluid collection, or other benign or malign pathologies based on CT attenuation values or morphological evaluation⁽²¹⁻²³⁾. However, the specific CT appearance of an air-filled spontaneously evacuated SAC within the granulation tissue renders it possible to differentiate it from other pathologies. The evacuated SAC may sometimes appear as a dry middle ear in advance stages, causing complete ossicular destruction (Figure 6).

Although tympanoplasty/atticotomy is a relatively elective operation in simple central or attic perforations/dry attic retraction pockets without cholesteatoma, the existence of cholesteatoma requires mastoidectomy. However, attic perforations/dry attic retraction pockets seen on clinical examinations could also simply represent a previously evacuated cholesteatoma with the outer wall left behind. This process would be underdiagnosed by an otologist as simple central or attic perforations/dry attic retraction pockets, and this underestimation may lead to further disease progression and a more extensive surgery. Also, particularly in cases where patients are not suitable for surgery (who have contraindication for general anesthesia or not willing to undergo surgery), differentiating between a deep retraction pocket and a drained cholesteatoma may be crucial. Additionally, with the inadequacy of magnetic resonance imaging in helping detect SAC in these cases, it is thus possible to say that in



Figure 4. a-c. Completely symmetrical coronal MDCT images of the temporal bone (a) show an auto-evacuated pars tensa cholesteatoma on the left side. Even if the opacification is evident in the lateral attic, ossicles are slightly displaced to the opacified side (arrow) compared with the contralateral side. There is slight ossicular erosion in the pathologic side in this case. In the axial image (b), smooth remodeling on the posterior wall and anterolateral displacement of the incus by circular empty cholesteatoma are seen (arrow). This image (c) is a magnified section of the left side temporal bone in (a) showing an auto-evacuated cholesteatoma.

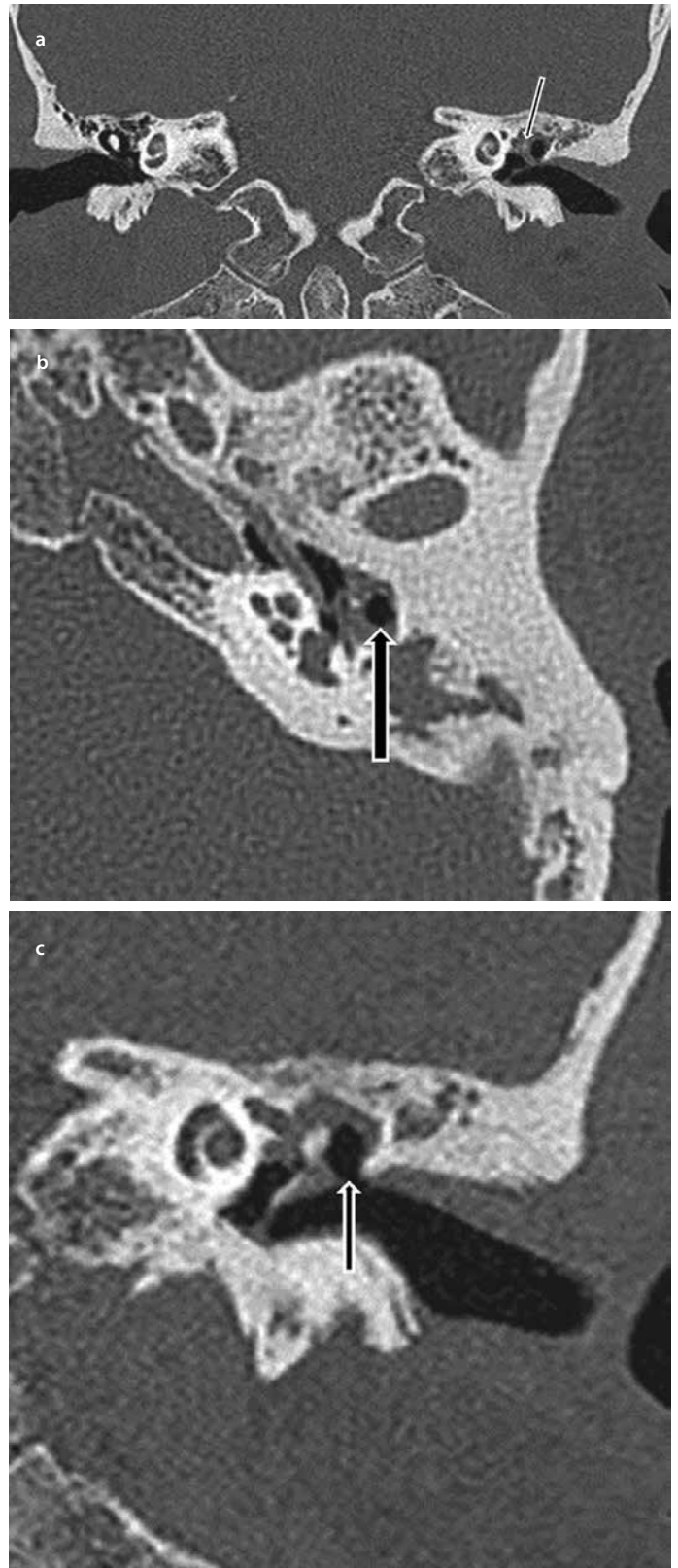


Figure 5 a-c. Completely symmetrical coronal MDCT images of the temporal bone (a) shows an auto-evacuated pars flaccida cholesteatoma on the left side. The body of incus is seen to be almost completely eroded and displaced medially (arrow). In the axial plane (b), a spherical air-filled cavity is seen inside the inflammation in the Prussak's space (arrow). In the coronal plane (c), it is clear that lateral attic is widened and the Shrapnell's membrane has lost its integrity (arrow), and the head of malleus and manubrium are intact.

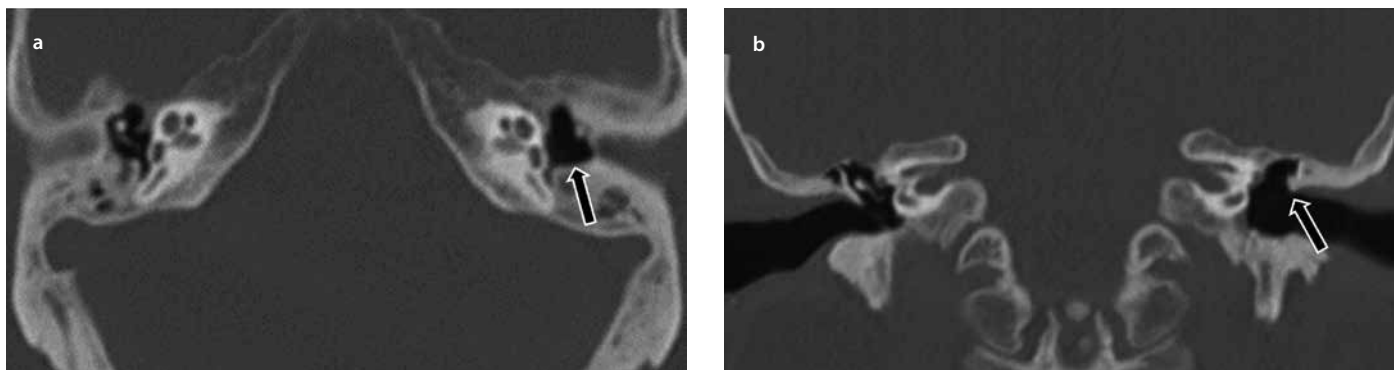


Figure 5. a, b. Completely symmetrical axial (a) and coronal (b) MDCT images of the temporal bone show no ossicle in the left middle ear. Smooth remodeling on the posterior wall in the axial plane (arrow in a) and scutum erosion in the coronal plane (arrow in b) are noted.

some circumstances, CT becomes determinative in the decision of the indication for surgery. Membrane retraction without a cholesteatoma leading to ossicular destruction has been also reported [21]. All of our patients were intraoperatively diagnosed with cholesteatoma. Clinically, otologists commonly decide on surgical treatment based on the patients' symptoms, e.g., discharge frequency, debris accumulation, and progressive conductive hearing loss, regardless of the presence of cholesteatoma. However, considering the potential of surgery to impair hearing, recurrence caused by residual squamous epithelium in the middle ear cavity after conservative surgery, or even worse, a combination of these two unwanted effects, the importance of the preoperative radiological evaluation of cholesteatoma becomes evident.

A cholesteatoma presenting as an aerated cavity instead of soft-tissue attenuation in the middle ear may lead to misdiagnosis in the CT follow-up investigations. In such situations, previous CTs and quantitative analyses may provide additional useful information for correct diagnosis. Since the distances evaluated were quite small, with large variation probable among patients, in our study, three different radiologists made the measurements in two separate planes at right angles. SAC of the middle ear is not histologically specific; therefore, the study depends on intraoperative observations to arrive at an appropriate diagnosis. These are the limitations of our study.

CONCLUSION

An auto-evacuated cholesteatoma should be considered when a temporal bone CT shows an expansive-looking air-filled structure within the granulation tissue, giving the impression of a cavity enclosed by a membranous wall with a smooth surface in the middle ear. Previous images showing a mass-like opacification in this location can support the diagnosis. In patients with a chronic aural discharge, evacuated cholesteatoma should be considered even if a temporal CT shows nonopacified aerated areas surrounded by granulation tissue, with or without destruction, and quantitative measurements should be made.

Key points:

Enlargement of the lateral attic can suggest pars flaccida cholesteatoma

Enlargement of the medial attic can suggest pars tensa cholesteatoma

Enlargement of the lateral or medial attic can be measurable on CT

Ethics Committee Approval: Ethics committee approval was received for this study from the ethics committee of Şişli Hamidiye Training and Research Hospital (No: 684, date: 06.21.2016).

Informed Consent: Written informed consent was obtained from patients who participated in this study.

Peer-review: Externally peer-reviewed.

Author Contributions: Concept – İ.Ç., G.B., A.S.M., U.G.; Design - İ.Ç., G.B.; Supervision İ.Ç., G.B., A.S.M.; Resources - A.S.M., U.G.; Materials - G.B., A.S.M., U.G.; Data Collection and/or Processing - İ.Ç., G.B., A.S.M.; Analysis and/or Interpretation - İ.Ç., G.B., A.S.M., U.G.; Literature Search - İ.Ç., G.B., U.G.; Writing Manuscript - İ.Ç., G.B.; Critical Review - İ.Ç., G.B.; Other - İ.Ç., G.B., A.S.M., U.G.

Conflict of Interest: The authors have no conflict of interest to declare.

Financial Disclosure: The authors declared that this study has received no financial support.

REFERENCES

- Swartz JD, Hagiwara M. Temporal bone: inflammatory disease. In: Som PM., Curtis HD, eds. Head and Neck Imaging. 5th ed. St. Louis, MO: Mosby, Elsevier; 2011: 1201-7. [CrossRef]
- Ferlito A, Devaney KO, Rinaldo A, Milroy CM, Wenig BM, Iurato S, et al. Clinicopathological consultation. Ear cholesteatoma versus cholesterol granuloma. *Ann Otol Rhinol Laryngol* 1997; 106: 79-85. [CrossRef]
- Olszewska E, Wagner M, Bernal-Sprekelsen M, Ebmeyer J, Dazert S, Hildmann H, et al. Etiopathogenesis of cholesteatoma. *Eur Arch Otorhinolaryngol* 2004; 261: 6-24. [CrossRef]
- Du Verney JG. *Traité de l'organe de l'ouïe [Treatise of the hearing organ]*. Paris: Bibliothèque interuniversitaire de médecine, 1683.
- Cruveilhier J. *Anatomie pathologique du corps humain*. Paris: J. B. Bailliere, 1829.
- Müller. Progress of the anatomy and physiology of the nervous system during the year 1836. *Br Foreign Med Rev* 1838; 5: 293-300.
- Kazahaya K, Potsic WP. Congenital cholesteatoma. *Curr Opin Otolaryngol Head Neck Surg* 2004; 12: 398-403. [CrossRef]
- Chole RA, Sudhoff HH. Chronic otitis media, Mastoiditis, and Petrositis. In: Flint PW, Haughey BH, Lund BJ, et al. editors. *Cummings, Otolaryngology, Head & Neck Surgery*. 5th ed. Mosby. 2010. [CrossRef]
- Martins O, Victor J, Selesnick S. The relationship between individual ossicular status and conductive hearing loss in cholesteatoma. *Otol Neurotol* 2012; 33: 387-92. [CrossRef]
- Olsen JM, Ribeiro Fde A, Yasui MM, dos Santos IT. Hearing loss assessment in primary and secondary acquired cholesteatoma. *Braz J Otorhinolaryngol* 2015; 81: 653-57 [CrossRef]

11. Nemzek WR, Swartz JD. Temporal bone: Inflammatory disease. *Head and Neck Imaging*. 5th ed. St. Louis, MO: Mosby. 2011.p.1190.
12. Gaurano JL, Joharjy IA. Middle ear cholesteatoma: characteristic CT findings in 64 patients. *Ann Saudi Med* 2004; 24: 442-7. [\[CrossRef\]](#)
13. Baráth K, Huber AM, Stämpfli P, Varga Z, Kollias S. Neuroradiology of cholesteatomas. *AJNR Am J Neuroradiol* 2011; 32: 221-9. [\[CrossRef\]](#)
14. Schwartz JD, Harnsberger HR. The Middle Ear and Mastoid. In: Schwartz JD, Harnsberger HR, eds. *Imaging of the Temporal Bone*. 3rd ed. New York: Thieme, 1998.p.87-107.
15. Lee SK, Yeo S, Park M, Byun J. Clinical analysis of 22 cases with automastoidectomy caused by cholesteatoma. *Int Adv Otol* 2013; 9: 232-9.
16. Manasawala M, Cunnane ME, Curtin HD, Moonis G. Imaging findings in auto-atticotomy. *AJNR Am J Neuroradiol* 2014; 35: 182-5. [\[CrossRef\]](#)
17. Soldati D, Mudry A. Knowledge about cholesteatoma, from the first description to the modern histopathology. *Otol Neurotol* 2001; 22: 723-30. [\[CrossRef\]](#)
18. Strunk CL. Cholesteatoma. In: Bailey BJ, Johnson JT, Newlands SD, eds. *Head and neck surgery--otolaryngology*. 4th ed. Philadelphia: J.B. Lippincott, 1993.p.2041-51.
19. Nardis PF, Teramo M, Giunta S, Bellelli A. Unusual cholesteatoma shell: CT findings. *J Comput Assist Tomogr* 1988; 12: 1084-85. [\[CrossRef\]](#)
20. Leighton SE, Robson AK, Anslow P, Milford CA. The role of CT imaging in the management of chronic suppurative otitis media. *Clin Otolaryngol Allied Sci* 1993; 18: 23-9. [\[CrossRef\]](#)
21. Borgstein J, Gerritsma TV, Bruce IA. Erosion of the incus in pediatric posterior tympanic membrane retraction pockets without cholesteatoma. *Int J Pediatr Otorhinolaryngol* 2008; 72: 1419-23. [\[CrossRef\]](#)
22. Phelps PD, Wright A. Imaging cholesteatoma. *Clin Radiol* 1990; 41: 156-62. [\[CrossRef\]](#)
23. Leighton SE, Robson AK, Anslow P, Milford CA. The role of CT imaging in the management of chronic suppurative otitis media. *Clin Otolaryngol Allied Sci* 1993; 18: 23-9. [\[CrossRef\]](#)